

Simulating storm surge waves for structural vulnerability estimation and flood hazard mapping

Adam Hatzikyriakou¹  · Ning Lin¹

Received: 30 November 2016 / Accepted: 18 July 2017 / Published online: 25 July 2017
© The Author(s) 2017. This article is an open access publication

Abstract Wave action during storm surge is a common cause of building damage and therefore a critical consideration when estimating structural vulnerability and mapping flood risk. Traditional depth-damage curves, however, relate building vulnerability solely to inundation depth and therefore neglect an important damage mechanism. Similarly, flood mapping studies typically emphasize expected inundation rather than wave conditions. In this study, we consider the impact of wave effects on vulnerability estimation and flood mapping using a pair of hydrodynamic models (ADCIRC + SWAN and BOUSS1D) to simulate inland storm surge flooding. The models are used to simulate flooding in a heavily impacted coastal community (Ortley Beach, New Jersey) during Hurricane Sandy (2012) and to estimate inland hazard parameters characterizing inundation, wave and velocity effects. To quantify structural vulnerability, fragility curves are developed by statistically relating the simulated hazard parameters to surveyed building damage. The results indicate that dynamic hazard characteristics such as significant wave height are the dominant predictors of severe structural damage. The flood simulation is also used to map the variation of surge and wave effects in the community. Comparing this analysis to flood zones delineated by the Federal Emergency Management Agency in the community's Flood Insurance Rate Map reveals severe wave action and building damage in a significant portion of the community deemed least exposed to flood impact. It is suspected that this misrepresentation of risk resulted from overconfidence in the performance of the community's frontal dune under severe surge and wave actions.

Keywords Storm surge · Structural vulnerability · Flood mapping · Waves · FEMA · FIRM

✉ Adam Hatzikyriakou
ah7@princeton.edu

Ning Lin
nlin@princeton.edu

¹ Department of Civil and Environmental Engineering, Princeton University, Engineering Quad, Princeton, NJ 08540, USA

1 Introduction

More than 6.6 million homes in the USA, valued at nearly \$1.5 trillion, are at risk of storm surge damage (Botts et al. 2015). This significant exposure to losses is compounded by expected increases in surge flooding due to sea level rise and climate change. In places like New York City, these combined effects are expected to change a 400-year flood event like Hurricane Sandy to a 20–130-year event by the end of the century (Lin et al. 2016). Given this widespread and increasing risk, accurately assessing storm surge impact is essential. Two important steps for doing so are estimating structural vulnerability and mapping flood hazards.

1.1 Structural vulnerability estimation

Estimating structural vulnerability consists of relating a building's performance during storm surge to its exposure to flooding. This has traditionally been treated using depth-damage curves which give the expected loss in a building's economic value as a function of flood inundation depth (Davis et al. 1988). The most common approach for constructing such curves is by empirically relating post-event surveys of damaged structures to their estimated inundation depth using observed highwater marks (Davis and Skaggs 1992). Frequently used depth-damage curves include those developed by Federal Insurance Administration (FIA), which are the basis of the popular flood loss model HAZUS (Davis and Skaggs 1992; Scawthorn et al. 2006). Depth-damage curves have been pivotal for estimating structural vulnerability and are essential for quantitative storm surge risk assessment. Recent applications include predicting future flood losses due to climate change in major coastal cities (Hallegatte et al. 2013) and performing cost–benefit analyses of flood mitigation strategies (Aerts et al. 2014).

Quantifying structural vulnerability using depth-damage curves, however, can be problematic in several respects. First, highwater marks used as proxies for the maximum water level at a structure are invariably sparse and can introduce large uncertainties into vulnerability estimation. Second, interpreting this maximum water level is frequently ambiguous. Whereas for slow-rise flooding (e.g., riverine and pluvial floods) highwater marks are typically characteristic of stillwater inundation, highwater marks during storm surge include the variable contribution of waves and flood velocity. Since wave and hydrodynamic loads on coastal structures are often orders of magnitude greater than hydrostatic loads (FEMA 2011), two structures with the same inundation depth can have considerably different damage responses depending on the relative magnitude of these dynamic effects. As a result, ignoring wave action and flood velocity may significantly misrepresent a structure's performance during storm surge, particularly if the primary concern is estimating structural damage losses as opposed to content losses.

To overcome these challenges, studies of recent surge events have used hindcast simulations of inland flooding as the basis for vulnerability estimation. One of the first such studies was an analysis of building damage on the Bolivar Peninsula during Hurricane Ike (2008), which confirmed that wave height and the associated slamming load were important predictors of building collapse (Tomiczek et al. 2014). Additional studies of Hurricane Sandy using a high-resolution inundation model determined that the depth-averaged velocity was also a significant damage predictor (Tomiczek et al. 2017). These results parallel similar studies of tsunamis, which have used numerical models to construct fragility curves based on flow velocity and hydrodynamic loads (Suppasri et al. 2011). Despite this progress, however, a formal framework for simulating flooding locally at a

structure and extracting relevant hazard predictors when estimating structural vulnerability remains to be proposed.

1.2 Flood hazard mapping

In addition to estimating structural vulnerability, accurately modeling inland storm surge flooding is also a fundamental step in flood hazard mapping. As the primary tool for communicating flood exposure, flood maps quantify the spatial variation of flood effects. Combining such maps with the estimated vulnerability of buildings to damage can be used to determine the risk storm surge poses to the built environment. In the USA, flood mapping dictating insurance premiums which ideally reflect this risk is governed by the Federal Emergency Management Agency (FEMA) through its National Flood Insurance Program (NFIP) (Crowell et al. 2007). Flood Insurance Rate Maps (FIRMs) delineate flood risk by defining flood zones based on the estimated 100-year base flood elevation (BFE). Since the NFIP's inception, FIRMs have served as an important mechanism for motivating flood mitigation in the over 20,000 communities participating the program (Wetmore et al. 2016).

With the NFIP running a deficit of \$23 billion in 2015, however, the inability of FIRMs to consistently reflect flood risk is apparent (Government Accountability Office 2015). Since wave action is a common cause of building damage, these mapping errors may be partly attributable to the treatment of waves in FIRMs. First, inland wave conditions in FIRMs are estimated using FEMA's Wave Height Analysis for Flood Insurance Studies (WHAFIS) model which has yet to be sufficiently validated (National Research Council 2009). One source of uncertainty is that wave conditions in WHAFIS are not treated probabilistically but rather assumed to occur during the 100-year surge event (Divoky et al. 2005). This decoupling of surge and wave may lead to either an overestimation or underestimation of inland flood elevations (National Research Council 2009). How these surge and wave effects are communicated in FIRMs is likewise problematic, with base flood elevations and especially wave conditions specified in low spatial resolutions. In the case of the highest risk VE flood zone, for example, the only wave guidance provided is to expect wave heights greater than 3 feet (Hatheway et al. 2005). Finally, the impact of waves on coastal defenses such as dunes has yet to be satisfactorily resolved. FEMA currently deems dunes as ineffective barriers only if their cross-sectional area above the 100-year stillwater elevation and seaward of the dune crest is less than 540 square feet (FEMA 2002).

Accurately modeling and communicating the spatial variation of inland waves using advances in hydrodynamic modeling is an essential step toward more robust flood hazard mapping. An important application of this modeling is mapping inland flooding from a historical event at a particular coastal community. Comparing such a hindcast simulation to the flood zones from the community's FIRM provides an important opportunity to evaluate the performance of FEMA's flood mapping procedure. Although historical events may not correspond with the 100-year base flood event reflected in FIRMs, this comparison nevertheless can be used to assess the relative performance of flood zones in reflecting flood risk. Previous comparisons of FEMA flood zones to assessed building damage have revealed cases of considerable mismatch between mapped and actual flood risk. A recent example and focus of this study includes an analysis for Ortley Beach, New Jersey, which was heavily impacted by storm surge during Hurricane Sandy. Following a survey of the community, Xian et al. (2015) noted a majority building damage in Ortley Beach was concentrated in a low-risk flood zone deemed by FEMA as the least susceptible to flooding.

Given such discrepancies, investigating potential inadequacies in FEMA's flood mapping procedures and better resolving inland flooding using hydrodynamic simulations is critically needed.

1.3 Objectives

In this study, we consider the impact of wave action on structural vulnerability estimation and flood hazard mapping by using a detailed study of building damage in Ortley Beach, New Jersey, during Hurricane Sandy (described in Sect. 2). To do so, a pair of hydrodynamic models is proposed and validated for efficiently simulating inland flooding (Sect. 3). The first is the coupled ADvanced CIRCulation and Simulating WAVes Nearshore model (ADCIRC + SWAN), which is used to simulate the large-scale evolution of surge and waves as a storm approaches the coast (Sect. 3.1.1). The second is a one-dimensional Boussinesq wave model (BOUSS1D), which is used to simulate nearshore and inland wave propagation (Sect. 3.1.2). The modeling framework is used to hindcast flood conditions in Ortley Beach during Sandy from which variables characterizing inland hydrostatic, wave and hydrodynamic effects are extracted (Sect. 4). In order to quantify structural vulnerability, fragility curves are developed by statistically relating these hazard parameters to surveyed building damage (Sect. 5). Finally, the hindcast simulation is used to map the spatial variation of inundation and wave action in Ortley Beach. This mapping is compared to the flood zones from the community's FIRM to evaluate the performance of FEMA's flood mapping procedure (Sect. 6).

2 Study event and location

2.1 Hurricane Sandy

Hurricane Sandy was a late-season tropical cyclone which significantly impacted coastal communities across the eastern USA with devastating storm surge. Although making its final landfall near Brigantine, New Jersey, on October 29, 2012, as a relatively weak post-tropical cyclone, several factors contributed to Sandy's unprecedented surge levels. In the days prior to landfall, Sandy grew dramatically in size as it underwent extratropical transition while drawing baroclinic energy from the temperature difference between its warm core and cold air from a mid-latitude trough (Halverson and Rabenhorst 2013). This increase in size coincided with an unusual westward track caused by an area of high pressure over Greenland blocking eastern movement (Mattingly et al. 2014). These unique meteorological phenomena, compounded with landfall during an unusually high astronomical tide, contributed record water levels across New Jersey and New York. At The Battery in New York City, for example, a record high storm tide elevation of 3.43 m above NAVD88 (North American Vertical Datum of 1988) was measured (McCallum et al. 2013). (NAVD88 is the predominant vertical datum used in the USA for referencing elevation data.) Sandy's track and storm tide measurements collected by the US Geological Survey (USGS) are shown in Fig. 1 (McCallum et al. 2013). In contrast to extensive flooding, maximum sustained wind speeds of only 80 mph (130 km/h) or less were measured at landfall. As a result, Sandy was not a design wind event and minimal wind-related damage to structures was observed (FEMA 2013).

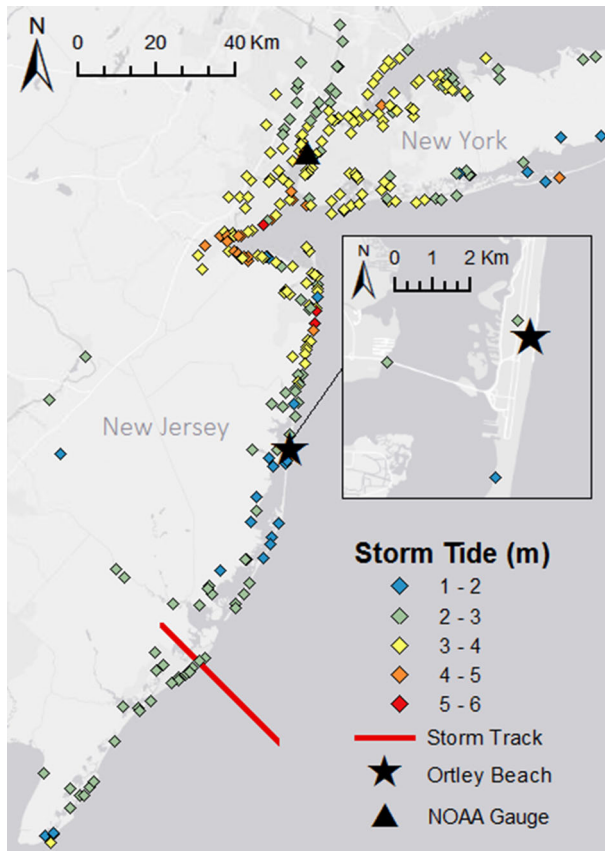


Fig. 1 Storm tide measurements from Hurricane Sandy (combined storm surge and astronomical tide above NAVD88) collected by the US Geological Survey using a temporarily deployed sensor network, permanent tide gauges and highwater mark observations. The *star marker* indicates the location of Ortlely Beach, New Jersey. The *triangle marker* indicates the location (40.70 N 74.01 W) of the NOAA gauge station used to evaluate ADCIRC + SWAN

2.2 Ortlely Beach

The impact of coastal flooding due to Sandy’s storm surge was devastating and responsible for a majority of the 650,000 structures damaged or destroyed during the cyclone (Blake et al. 2013). One of the hardest-hit areas was Ortlely Beach, New Jersey, a residential community comprised of single- and two-story light-frame wood structures with an average construction date around 1965. Located on a low-lying barrier peninsula (Fig. 1 inset), Ortlely Beach experienced significant inundation during Sandy with a USGS high-water mark measurement in the community recording a storm tide of 2.65 m above NAVD88 (McCallum et al. 2013). This substantial flooding was primarily a consequence of the near-total erosion of the community’s coastal dune (FEMA 2013). Erosion was so severe that in certain locations the dune’s peak elevation decreased by as much as 3 m, or 50% of its original height (Hatzikyriakou et al. 2015). The resulting surge overtopping and inland flooding caused significant damage to structures in the community, with only the foundation footprint remaining for many buildings. Out of 2772 applicants for FEMA

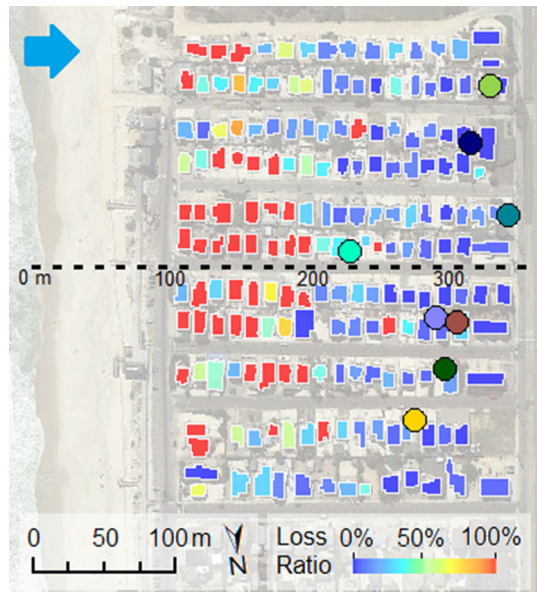
assistance in Ortley Beach, 284 (10%) experienced losses greater than \$30,000 (O’Dea 2013).

Following Hurricane Sandy, a team of students and faculty from Princeton University and the University of Notre Dame surveyed buildings in the most impacted portion of the community (Hatzikyriakou et al. 2015). Using photographs of each surveyed structure, Xian et al. (2015) assessed physical damage to critical building components such as foundations, exterior walls, exterior siding, windows and doors. Combining these damage assessments with the replacement cost of each component estimated using the RS Means (2013) online database, Xian et al. (2015) computed a loss ratio giving the percent loss in a structure’s overall economic value. Figure 2 shows a plan view of Ortley Beach with each polygon representing the footprint of a surveyed building shaded according to its assessed loss ratio. The direction of the surge is illustrated by the blue arrow. As illustrated in the figure, structures near the coast were the most impacted by flooding, with buildings further inland experiencing lower losses. The following two sections present a framework for hindcasting coastal flooding during Sandy (Sect. 3) and characterizing the inland flood conditions experienced by structures (Sect. 4).

3 Storm surge simulation

Storm surge is a multi-scale phenomenon which spans cyclone development all the way to inundation locally at a structure. To capture this complicated evolution, the hydrodynamic modeling used in this study is divided into two levels. The first level consists of the coupled ADvanced CIRCulation and Simulating WAVes Nearshore models (ADCIRC + SWAN; Dietrich et al. 2011) for simulating Sandy’s surge/wave evolution beginning 6 days prior to landfall. Outputs from this coupled model are in turn used to

Fig. 2 Plan view of Ortley Beach, New Jersey, with polygons representing surveyed buildings (189 in total) shaded according to their assessed loss ratio. *Colored circular markers* represent the location of observed highwater marks referred to in Fig. 4. The *dashed line* marked with its length in meters represents a cross-sectional transect of the community referred to in Figs. 5, 9 and 10. Loss data were obtained from Xian et al. (2015)



simulate coastal run-up and inland flood inundation using a one-dimensional phase-resolving Boussinesq surf zone model (BOUSSID; Demirbilek et al. 2009).

3.1 Hydrodynamic models

3.1.1 ADCIRC + SWAN

The ADCIRC + SWAN model uses the moving wind and pressure field of a tropical cyclone as forcing to simulate the associated time-varying surge/wave conditions (Dietrich et al. 2011). ADCIRC computes water levels and currents by solving the shallow water and momentum equations on an unstructured finite element grid (Luettich et al. 1992). Wave propagation is modeled at each time step using SWAN by solving the wave action balance equation (Booij et al. 1999). Since resolving the phases of individual waves over very large domains is computationally infeasible, waves in SWAN are phase-averaged so that wave statistics rather than the actual sea surface are determined at each time step. The coupled ADCIRC + SWAN model has been extensively validated with historical cyclones including Gulf Coast events such as Hurricanes Katrina (2005) and Ike (2008) (Dietrich et al. 2012). The model has likewise become the basis for flood risk mapping by FEMA (2014b).

3.1.2 BOUSSID

Estimating the flood exposure of structures within a community requires modeling wave run-up (i.e., uprush of water on a slope following wave breaking), wave overtopping (i.e., the rate of run-up over the crest of a beach) and inland inundation. Since both ADCIRC and SWAN are large-scale hydrodynamic models used to simulate storm surge evolution along the coast, resolving meter-length coastal features such as dune profiles is computationally infeasible. Furthermore, the phase-averaging of waves in the coupled ADCIRC + SWAN model can underestimate inundation since individual wave crests within a wave group can penetrate significantly further inland (Kennedy et al. 2012). Due to these limitations, the National Research Council (2009) in its review of storm surge modeling in the USA has recommended greater use of two-dimensional phase-resolving models for inland flood simulations. Boussinesq-type models capable of handling complex topographies and capturing individual wave crests offer an attractive means of doing so. A recent application of a two-dimensional Boussinesq model includes a hindcast study of flooding in Ortley Beach during Hurricane Sandy used to estimate building vulnerability (Tomiczek et al. 2017).

Although two-dimensional Boussinesq models provide detailed information on inland flooding, their high computational cost makes simulating flooding for a large number of events or over a large study area infeasible. Furthermore, for communities like Ortley Beach which are nearly uniform in the longshore direction, two-dimensional models provide limited additional insight compared to one-dimensional models. As a result, a simplified and computationally efficient one-dimensional Boussinesq phase-resolving model (BOUSSID; Demirbilek et al. 2009) is used and evaluated in this study. The model has previously been used to simulate surge inundation from tropical cyclones in the Hawaiian Islands of Oahu and Kauai (Kennedy et al. 2012). Due to its computational efficiency, it is likewise used by Taflanidis et al. (2013) to pre-simulate inundation for a large parameter space of hurricane characteristics in order to develop surrogate surge models for rapid surge prediction during an event.

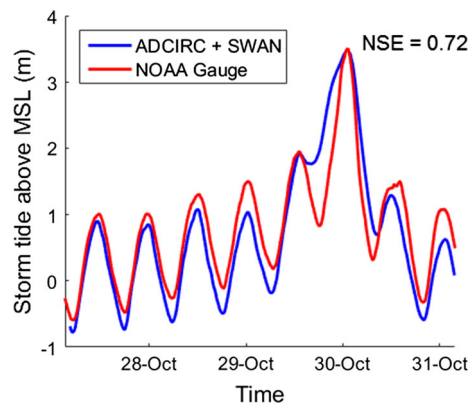
3.2 Model implementation and evaluation

A hindcast of Sandy's surge was simulated with ADCIRC + SWAN using a computational mesh and bathymetric data developed by the Region II office of FEMA (FEMA 2014b). The mesh has a ~ 100 -m resolution near the coast and ~ 50 -km resolution over the deep ocean. The modeling was driven by surface wind, sea level pressure and tidal forcing following an approach similar to Yin et al. (2016). Tidal forcing was applied at the open boundary by eight tidal constituents (K1, K2, M2, N2, O1, P1, Q1 and S2). A parametric approach was used to simulate Sandy's wind and pressure at each grid point based on storm characteristics (center location, maximum wind speed, minimum central pressure and radius of maximum wind) obtained from the Extended Best Track database (Demuth et al. 2006; updated). Specifically, sea level pressure was estimated from a simple parametric model (Holland 1980) and surface wind was estimated by fitting the wind velocity to a symmetrical hurricane wind profile (Chavas et al. 2015) and adding a fraction (0.55 at 20° cyclonically) of the storm translation velocity to account for the asymmetry of the wind field induced by the surface background wind (Lin and Chavas 2012).

The ADCIRC + SWAN simulation is evaluated by comparing simulated storm tide above mean sea level to observed water level measurements from NOAA gauge station #8518750 located at The Battery in New York City (Fig. 3). The time histories show good agreement, with a Nash–Sutcliffe efficiency (the ratio of the mean square error to the variance of the observed data subtracted from unity) of 0.72. The slight discrepancy in the tidal peaks before and after the maximum storm tide level on October 30, 2012, is likely a result of the simple parametric analysis of Sandy's wind profile which did not treat the extratropical and hybrid characteristics of the storm. The simulation, however, agrees well with the observed maximum storm tide of 3.5 m above mean sea level, which is likely to be the controlling factor of inland flooding.

BOUSSID is implemented using one-dimensional cross-shore transects of Ortley Beach originating a kilometer offshore. The ground elevation along transects is extracted at a 2-m grid spacing from a Light Detection and Ranging (LiDAR) survey of the New Jersey coast conducted by the USGS immediately following Hurricane Sandy (Wright et al. 2014). The post-Sandy elevation is used in order to consider the impact of dune erosion on inland flooding. Since accounting for the effect of buildings in the large study area is not numerically possible given existing methods, a bare-earth topography with buildings removed is used. Although this simplification does not capture the potential dampening of

Fig. 3 Comparison of ADCIRC + SWAN simulated storm tide above mean sea level (m) and observed water levels at NOAA gauge station #8518750 located at The Battery, New York. The location of the gauge station is shown as a *triangle marker* in Fig. 1. The computed Nash–Sutcliffe efficiency (NSE) is also indicated

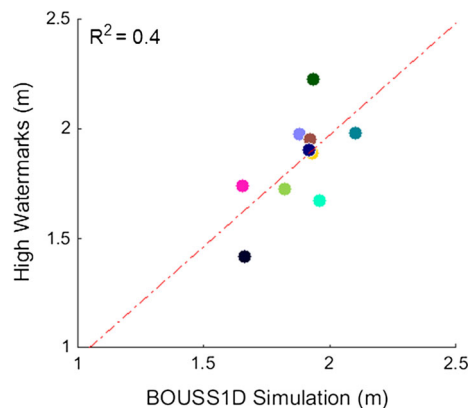


waves due to flood obstructions, it nevertheless provides an informative and computationally feasible means of simulating inland flooding. Hydrodynamic forcing for each transect is specified at its origin using an irregular wave generation based on the parametric Joint North Sea Wave Project (JONSWAP) wave spectrum (Hasselmann et al. 1973). The wave spectrum is defined using the peak surge level, significant wave height and maximum wave period at the transect origin estimated from the ADCIRC + SWAN simulation. The model is run during the half hour of maximum surge, with a computational run time of approximately 2 min for each simulation using a desktop computer. At the end of the simulation, time histories of inundation and additional surge parameters are extracted at points of interest along each transect.

The BOUSS1D model is evaluated by comparing observed highwater marks in the community with simulated inundation. Highwater marks are debris lines or water stains on stationary objects indicating the maximum water elevation during a flood. Highwater mark heights (also known as trace heights) in Ortley Beach were collected using a mobile LiDAR survey of the community following Sandy (Hatzikyriakou et al. 2015). Mobile LiDAR systems comprise cameras and laser-emitting sensors mounted on a vehicle, which are capable of collecting highly accurate spatial point clouds. The locations of collected highwater marks are shown as colored circles in Fig. 2. Highwater marks tended to be observed in areas with low structural damage since it was difficult to distinguish debris lines or water stains on heavily damaged or totally destroyed structures. A comparison of highwater mark heights above ground level and the maximum simulated water elevation above ground level at their respective locations is shown in Fig. 4. The comparison shows relatively good agreement considering the complexity of inland storm surge flooding, with an R^2 of 0.4. Further research, however, validating BOUSS1D in areas with more empirical data on flood conditions would be valuable.

In order to quantify structural vulnerability, the ADCIRC + SWAN and BOUSS1D modeling framework is first used to simulate flooding at each of the surveyed structures in Ortley Beach. To do so, cross-shore transects are first generated every 20 m along the shore. The centroid of each structure's footprint is next projected onto the nearest transect, representing the location at which storm surge parameters are extracted. In order to map the spatial variation of flood effects in the community, storm surge parameters are also extracted at 5-m intervals along a single transect shown as a dashed line in Fig. 2. The following section details the storm surge parameters extracted from the simulations.

Fig. 4 Comparison of surveyed highwater mark elevation above the ground and BOUSS1D simulated inundation. Note that the *color* of the data points corresponds to the *color* of markers in Fig. 2. Two watermarks, colored pink and black, are located beyond the extent of Fig. 2



4 Storm surge parameters

4.1 Fundamental parameters

Storm surge impact on coastal structures can be categorized into three principle effects—(1) hydrostatic effects due to standing water against a structure, (2) wave action due to wave breaking and (3) hydrodynamic effects due to surge rapidly flowing around a structure (FEMA 2011). These effects can, respectively, be characterized by the inundation depth, wave height and surge flow velocity locally at a structure. From the hindcast simulation of Hurricane Sandy, a time history of inundation depth (i.e., the water level above the ground, $d(t)$), is first extracted at each point of interest. A zero down-crossing analysis of the inundation time series is used to determine wave heights over the simulation time (Forristall 1978). Finally, time histories of the depth-averaged velocity, denoted as $u(t)$, are obtained. (Overland flooding consists mainly of shallow water conditions with velocity nearly constant with depth.)

4.2 Derived variables

Given the above fundamental surge parameters, several descriptive variables are derived as building damage predictors. The variables d_{\max} , $d_{75\%}$, d_{mean} , $d_{25\%}$ and d_{\min} are, respectively, defined as the maximum, 75th percentile, mean, 25th percentile and minimum inundation level above the ground over the half-hour simulation. To consider the effect of building elevation on damage, the relative inundation, d_{rel} , which is the difference between the maximum water level at a structure and its front door elevation is also determined. (The front door elevation for each structure was measured during the damage survey of Ortley Beach.) From the results of the zero-crossing analysis, maximum wave height (H_{\max}), the average of the highest third of waves (known as the significant wave height, H_{sig}), mean wave height (H_{mean}), the average of the highest tenth of waves ($H_{1/10}$) and minimum wave height (H_{\min}) are extracted. Finally, the variables u_{\max} , $u_{75\%}$, u_{mean} , $u_{25\%}$ and u_{\min} are, respectively, defined as the maximum, 75th percentile, mean, 25th percentile and minimum depth-averaged velocity at a structure.

Figure 5 shows the pre-/post-Sandy ground elevation (Fig. 5a) and the variation of these three surge effects (Fig. 5b–d) along the cross-shore transect of Ortley Beach shown as a dashed line in Fig. 2. As noted earlier and illustrated in Fig. 5a, the significant inundation in Ortley Beach was largely due to the erosion of the community's frontal dune. Peculiarly, however, although the damage in the community is greatest near the coast and decreases further inland (see Fig. 2), maximum inundation (red line in Fig. 5b) only slightly decreases over this region. Furthermore, other measures of inundation such as d_{mean} counterintuitively increase with distance inland. In contrast, wave action (Fig. 5c) and depth-averaged flood velocity (Fig. 5d) noticeably decay along the transect due to the dissipative effects of overland flooding. The spatial variability of these dynamic effects is more consistent with observed damage in Ortley Beach (Fig. 2), suggesting that wave action and hydrodynamic effects were the primary damage mechanisms.

Ortley Beach's topography (which decreases in elevation with distance from the coast; Fig. 5a) and the cross-shore decrease in waves help explain the unexpected inundation depths simulated in the community. The contribution of waves in nearshore locations and lower ground elevation further inland cancel to produce only a gradual decay of maximum

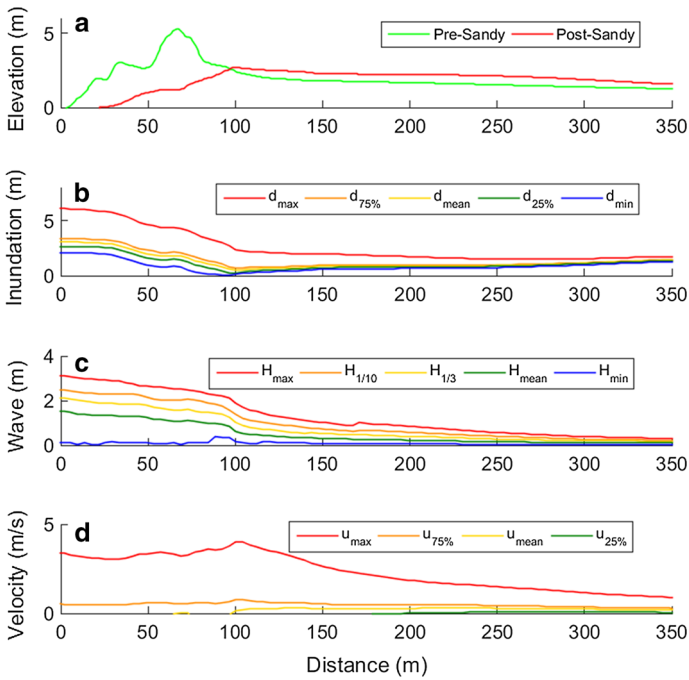


Fig. 5 **a** Ground elevation above NAVD88 before and after Hurricane Sandy, **b** surge inundation above ground level, **c** wave statistics and **d** depth-averaged velocity along the dashed transect shown in Fig. 2

inundation. In comparison, metrics of inundation such as d_{mean} which are less affected by wave action increase with distance inland as the ground elevation decreases.

4.3 Structural loads

In addition to describing storm surge parameters, it is also useful to directly estimate the flood loads on structures. Since wave action is typically the most destructive flood characteristic (FEMA 2011), in this section we discuss wave loads on closed foundations (the dominate construction type in Ortley Beach). Computing the total lateral load on a structure requires integrating distributed flood loads over the area of its seaward facing wall. To avoid the complexity of considering varying building geometries, we focus here on wave loads per linear width of a structure’s seaward wall.

Wave load calculation using FEMA’s Coastal Construction Manual is based on the depth-limited breaking wave height at a structure, taken as 0.78 times the stillwater flood depth (FEMA 2011). Based on this underlying assumption, FEMA’s suggested equation for computing wave loads is given by

$$F_{wave,FEMA} = 1.1C_p\gamma_w d_s^2 + 2.4\gamma_w d_s^2 \tag{1}$$

where γ_w is the specific weight of seawater, C_p is a dynamic pressure coefficient chosen based on the risk category of the structure (taken as 2.8 for residential buildings; see FEMA 2011; Walton et al. 1989), and d_s is the stillwater flood depth, which can be taken as the mean inundation d_{mean} . This load equation counterintuitively suggests the far-shore structures with higher stillwater depths (due to the gradually decreasing elevation of Ortley

Beach with distance from the coast) experienced larger wave loads than structures near the coast. This result is not supported by the simulated wave behavior or the surveyed damage in the community. As an alternative approach, Allsop et al. (1996) provide an equation for calculating impact wave loads as a function of significant wave height, H_{sig} , based on an experimental study of vertical breakwaters. The wave load equation is given by

$$F_{\text{wave,Allsop}} = 15 \left(\frac{H_{\text{sig}}}{d} \right)^{3.134} \rho g d^2 \quad (2)$$

where ρ is the mass density of seawater (1029 kg/m^3), g is the gravitational acceleration constant (9.81 m/s^2), and d is the water depth (taken as the mean inundation d_{mean}). The load equation is valid for values of H_{sig}/d less than 0.6. This threshold was satisfied for a majority of structures with the exception of several nearshore buildings which experienced significant wave action and which were therefore excluded from the analysis.

5 Quantitative vulnerability analysis

The preceding hindcast of flood conditions experienced by structures is next related to their surveyed loss ratios in order to empirically estimate structural vulnerability. This vulnerability estimation is approached from two perspectives. The first approach is to discretize a structure's loss ratio and then to determine the probability of a given damage state as a function of hazard predictors. For binary and ordinal damage states, this analysis, respectively, yields vulnerability and fragility curves. A second approach is to estimate the expected loss ratio of a structure as a function of hazard predictors. This analysis yields curves analogous to familiar depth-damage curves. Following a short presentation of both approaches, we fit the models and discuss the significance of various hazard parameters. We note functions for implementing each method in R, a common statistical software (R Development Core Team 2015).

5.1 Methods

To begin consider a random damage response, Y , and a vector of p explanatory variables, X . To be consistent with traditional approaches for estimating structural vulnerability, it is assumed that damage to nearby structures is not correlated due to interaction mechanisms such as waterborne debris. Hatzikyriakou and Lin (2016) discussed extensions of the subsequent methods for considering the correlation in damage responses, which would lead to higher statistical uncertainties (larger confidence intervals) for vulnerability estimates.

5.1.1 Probability approach

Consider Y as a discrete damage state. For a binary state coded 1 for failure and 0 for survival, the probability of observing failure, which is equivalent to the expectation of Y , can be related to X in a logistic regression

$$g = P[Y = 1|X] = E[Y|X] = \frac{e^{\alpha + X'\beta}}{1 + e^{\alpha + X'\beta}} \tag{3}$$

where α is a regression intercept and $\beta = (\beta_1, \dots, \beta_p)'$ is a vector of regression coefficients.

This probability of failure can be transformed into a linear predictor using a link function $\text{logit}(\cdot)$

$$\text{logit}(g) = \log \frac{g}{1 - g} = \alpha + X'\beta \tag{4}$$

In order to dichotomize loss ratios into a binary response, failure (survival) is defined according to whether a structure’s loss ratio is greater (less) than 50%. This criterion is chosen since FEMA requires that structures with ‘substantial damage’ following an event (defined as greater than 50% in market value) comply with current design standards (FEMA 2010). Given a sample of observed damaged states (y_1, \dots, y_n) and explanatory variables (x_1, \dots, x_n) for the n structures in the community, the regression parameters $\theta = (\alpha, \beta)'$ can be estimated using maximum likelihood. To do so, a likelihood function

$$\mathcal{L}(\theta) = \prod_{k=1}^n (g_k)^{y_k} (1 - g_k)^{1 - y_k} \tag{5}$$

can be constructed as the product of the Bernoulli-distributed likelihood of each observation. The likelihood function can be numerically maximized to obtain parameter estimates using the function `glm` in R. Confidence intervals for the failure probability can be calculated using estimates of the variance and covariance of the fitted coefficients.

The performance of a structure, Y , can also be characterized by multiple discrete damage states. For the purpose of this study, loss ratios are converted into five ordinal damage states based on cutoff values of 0.2, 0.4, 0.6 and 0.8. To preserve the ordered nature of the damage scale, the cumulative probability of a damage state $P[Y \leq d]$ can be related to covariates using a cumulative logit model, which is given by

$$P[Y \leq d|X] = \frac{e^{\alpha_d + X'\beta}}{1 + e^{\alpha_d + X'\beta}} \tag{6}$$

In this model, the effects of covariates on the damage response are assumed to be the same across all damage states, whereas the intercept $\{\alpha_d\}$ is allowed to differ (Agestri 2010). As with logistic regression, the regression parameters $\theta = (\{\alpha_d\}, \beta)'$ can be estimated using maximum likelihood (using `vglm` or `polr` in R).

5.1.2 Expectation approach

Consider Y as a loss ratio. Correctly estimating the expected loss of a structure for a given set of covariates, $E[Y|X]$, can face several challenges due to the bounded nature of loss ratios (i.e., $Y \in [0, 1]$). First, the convenient use of linear models for $E[Y|X]$ is not appropriate since they do not guarantee predictions in the unit interval. Furthermore, the clustering of data points at zero and one frequently creates problems of heteroscedasticity as the variance of responses is not constant across all values of covariates. One approach to dealing with fractional data is to first use a nonlinear transform to linearize the data and then to implement ordinary least squares (OLS) (Warton and Hui 2011). However, since

transformations are typically only asymptotically bounded within the unit interval, ad hoc adjustments of zero and one data are first needed, introducing bias into parameter estimation. Furthermore, additional steps are then needed to retransform OLS estimates into the original scale for interpretation (Ramalho et al. 2011). A more complicated alternative is to apply an inflated model which uses separate distributions for continuous data in the open $(0, 1)$ interval and the discrete zero and one data (Ospina and Ferrari 2008).

For this study, we use an easily implementable fractional logit model proposed by Papke and Wooldridge (1996). Unlike logistic regression which assumes that the response variable follows a Bernoulli distribution, the fractional logit model specifies only the conditional expectation of responses, $E[Y|X]$. In order to respect the boundedness of responses in the unit interval, the conditional expectation is chosen as a logistic function

$$h = E[Y|X] = \frac{e^{\alpha + X'\beta}}{1 + e^{\alpha + X'\beta}} \quad (7)$$

where α is a regression intercept and $\beta = (\beta_1, \dots, \beta_p)'$ is a vector of regression coefficients. Given a sample of observed loss ratios (y_1, \dots, y_n) and explanatory variables (x_1, \dots, x_n) , the regression parameters $\theta = (\alpha, \beta)'$ can be estimated by maximizing

$$\mathcal{L}(\theta) = \prod_{k=1}^n (h_k)^{y_k} (1 - h_k)^{1-y_k} \quad (8)$$

Although Eq. 8 is not a likelihood function, it can be shown that this quasi-likelihood approach yields consistent parameter estimates and robust standard errors (Papke and Wooldridge 1996). The statistical uncertainty in the estimated conditional expectation can be quantified using confidence intervals analogous to those from logistic regression. The model's goodness of fit can be specified by a coefficient of determination, R^2 , which is computed as the square of the correlation between the actual and fitted loss ratio responses (Ramalho et al. 2010).

5.2 Vulnerability curves

The fractional logit model is used to empirically develop damage curves quantifying structural vulnerability. These include a conventional depth-damage curve (Fig. 6a), a wave-damage curve (Fig. 6b) and a velocity-damage curve (Fig. 6c), which, respectively, relate maximum relative inundation, significant wave height and maximum depth-averaged velocity to a structure's expected loss ratio. The R^2 value for each fitted model is likewise shown in each plot.

Since there was little to no building elevation requirement for structures in Ortley Beach (see Sect. 6.2), a majority of structures in the community were elevated to around half a meter above the ground. With maximum inundation gradually decaying across the community, the water level relative to the lowest horizontal member of structures tended to only slightly decrease with distance from the coast. As a result, the depth-damage curve (Fig. 6a) shows a weak positive trend between relative inundation and loss ratio. This is quantified by a small R^2 value of 0.14. In contrast, both the wave-damage and velocity-damage curves show considerably better predictive power. In the case of the wave-damage curve, a relatively small increase in significant wave height from 0.2 to 0.4 doubles the expected loss ratio of a structure, highlighting the importance of considering wave action when designing structures.

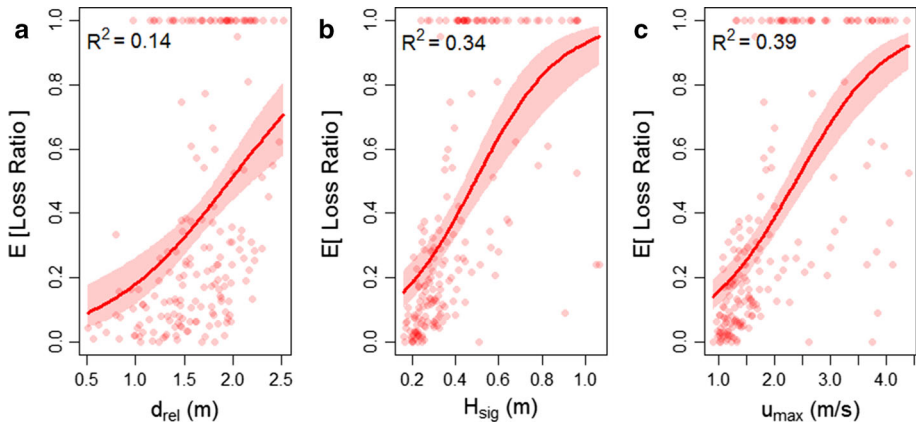


Fig. 6 Estimated **a** depth-damage, **b** wave-damage and **c** velocity-damage curves. *Solid lines* and *shaded regions*, respectively, represent the estimated expected loss ratio and the associated 95% confidence interval, with points representing the initial raw data

Wave effects are further explored by using the fractional logit model to relate estimated wave loads to surveyed building loss ratios. Wave loads are calculated using the methods presented by FEMA (Eq. 1; Fig. 7a) and by Allsop et al. (1996) (Eq. 2; Fig. 7b). A comparison of the two load-damage curves shows opposite trends, with building losses actually decreasing as a function of wave loads according to the FEMA approach. As noted earlier, this trend results from the assumption of depth-limited waves in the FEMA formulation. Wave loads computed using this approach are likewise significantly larger in magnitude, potentially due to the C_p coefficient acting as a safety factor. In contrast, the damage curve based on Allsop et al. (1996) is consistent with the expected relationship between wave loads and building damage. Furthermore, in comparison with the significant wave height damage curve shown in Fig. 6b, treating wave loads directly increases the predictive power R^2 of the damage curve from 0.34 to 0.47.

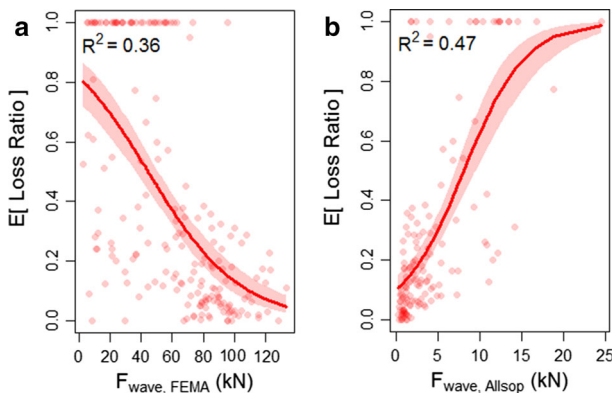


Fig. 7 Estimated load-damage curves based on the **a** FEMA and **b** Allsop et al. (1996) methods for computing wave loads. The *solid line* and *shaded region*, respectively, represent the estimated expected loss ratio and associated 95% confidence interval, with points representing the raw data

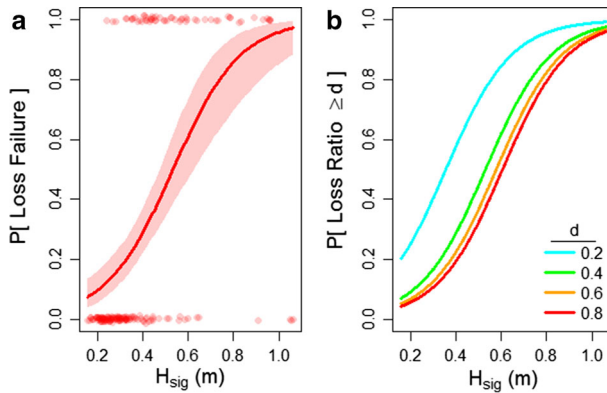


Fig. 8 **a** Vulnerability curve relating significant wave height to the probability of loss failure. The *solid line* and *shaded region*, respectively, represent the estimated probability of failure and associated 95% confidence interval, with points representing raw data. **b** Fragility curves relating significant wave height to the probability of equalling or exceeding a loss ratio of 0.2 (*blue*), 0.4 (*green*), 0.6 (*orange*) and 0.8 (*red*)

In addition to estimating the expected loss ratio of a structure, Fig. 8 illustrates the probability associated with particular damage states. First, the vulnerability curve in Fig. 8a shows the probability of experiencing loss failure (defined as a structure losing greater than 50% of its value) as a function of significant wave height. Consistent with the wave-damage curve, an increase in significant wave height from 0.2 to 0.4 m increases the probability of loss failure from 0.1 to 0.3. A similar trend is likewise found in the fragility curves shown in Fig. 8b, which relate significant wave height to the probability of exceeding a given loss ratio. For an increase in significant wave height from 0.2 to 0.4 m, the probability of equalling or exceeding a loss ratio 0.2 increases from 0.25 to 0.58.

6 Flood hazard mapping

In this section, the hindcast simulation of Sandy's flooding in Ortley Beach shown in Fig. 5 and discussed in Sect. 4 is used to evaluate the performance of FEMA's flood map in the community. As the primary tool for communicating flood exposure in the USA, flood mapping by the Federal Emergency Management Agency (FEMA) plays a fundamental role in many aspects of storm surge risk management (Merz et al. 2007).

6.1 Flood mapping in the USA

Flood hazard maps dictating insurance premiums and building design in the USA are governed by FEMA through its National Flood Insurance Program (NFIP). In order to communicate flood exposure, FEMA develops Flood Insurance Rate Maps (FIRMs) which classify coastal areas into flood zones based on two principal criteria. The first is the area's base flood elevation (BFE) representing the elevation of the estimated 100-year (i.e., 1% annual chance) flood event. The second criterion is the expected wave conditions associated with this event, specified as a range (e.g., 'greater than 3 feet'). One approach to evaluating FEMA's flood hazard mapping for a location is to compare it with simulated inland flooding from a historical event. Although it is estimated that Sandy's surge was on

the order of a 400-year event (Lin et al. 2016), comparing simulated flooding in Ortley Beach to the community's FIRM provides a unique opportunity to assess the relative performance of flood zones in accurately reflecting flood exposure. In one of the few such studies along these lines, an analysis of surge impact from Hurricane Iniki (1992) in Kauai, Hawaii, found considerable inconsistency between observed overwash and the 100-year flood extent determined by FEMA (Fletcher et al. 1995).

6.2 Evaluation of flood mapping in Ortley Beach

The first FIRM in Ortley Beach was released in 1979 and updated in 1983. The current effective FIRM was released in September 2006; however, it is based on the coastal analysis dating from the 1983 map (FEMA 2014a). A revised preliminary FIRM was released in January 2015 and is expected to be approved soon. Flood risk in the effective and preliminary Ortley Beach FIRMs is categorized into four flood zones typical of most communities (FEMA 2011; Hatheway et al. 2005). Design requirements in these zones apply to all newly constructed structures and to rebuilt structures where the cost of improving a building exceeds 50% of its market value.

- *VE Zone* subject to inundation by the 100-year flood event with wave heights equal to or greater than 3 feet. All structures must have an open pile foundation elevated to or above the specified BFE.
- *AE Zone* subject to inundation by the 100-year flood event with wave heights less than 3 feet. Structures can have either open foundations or closed foundations (with openings) elevated to or above the specified BFE.
- *AO Zone* subject to inundation by the 100-year shallow flooding event (i.e., flooding due to a lack of channels allowing for drainage) where average depths are between 1 and 3 feet. The average flood depth rather than a BFE is specified in the FIRM. The lowest horizontal member of structures must be elevated to at least the average flood depth.
- *Shaded X Zone* subject to inundation by the 500-year flood event. No BFE specified and there are no minimum elevation requirements for structures.

Figure 9 shows the comparison of the hindcast simulation of storm surge to flood zones from Ortley Beach's effective FIRM along the dashed transect shown in Fig. 2. Specifically, Fig. 9a shows the comparison of flood zone BFE elevations to simulated inundation metrics above NAVD88 analogous to those discussed in Sect. 4.2. Similarly, Fig. 9b shows the comparison of flood zone wave requirements to simulated wave characteristics. Although these comparisons are based on a single transect, flood zones in both the effective and preliminary flood maps (Fig. 10) are nearly constant in the longshore direction.

As illustrated in Fig. 9a, flood risk in the effective FIRM for Ortley Beach is classified into three categories—two high-risk VE Zones seaward of the coastal dune, a moderate-risk X Zone in the area 100 m inland of the dune and a high-risk AE Zone covering the rest of the community. Maximum inundation along the transect significantly exceeded FEMA's 100-year flood levels, particularly for the X Zone where no BFE is specified and in the AE Zone where the BFE is close to the ground level. More significantly, the unexpected placement of the lower-risk X Zone between the high-risk VE and AE zones implies a strong discontinuity in flood risk, which is not seen in the inundation hindcast. This is especially true in the comparison of flood zone wave requirements to simulated wave effects shown in Fig. 9b. Although expected wave conditions in the VE Zones (i.e., greater

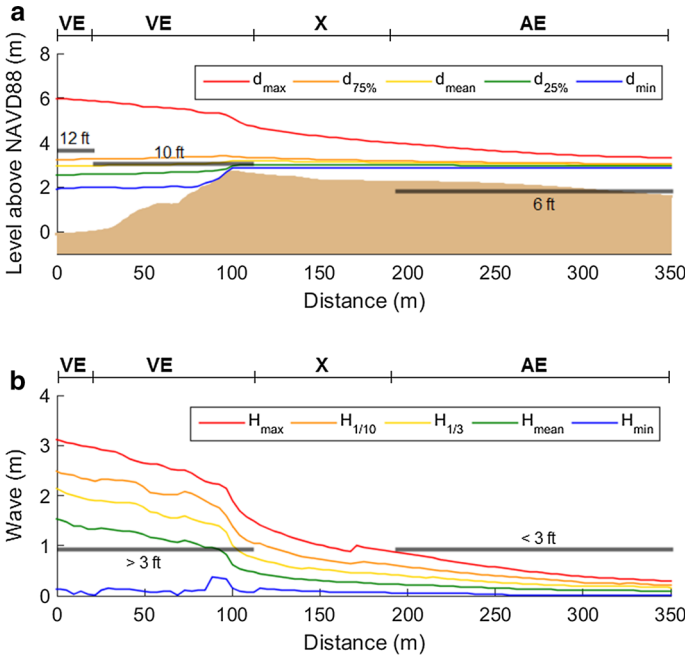


Fig. 9 Comparison of the hindcast simulation along the dashed transect shown in Fig. 2 to the effective FIRM in Ortley Beach. **a** Comparison of simulated inundation metrics to flood zone BFEs shown as horizontal black lines. The shaded brown area represents the transect’s post-Sandy ground elevation. **b** Comparison of simulated wave statistics to flood zone wave conditions

than 3 feet) and AE Zone (i.e., less than 3 feet) reflect wave effects during Sandy, significant wave action is not represented by the X Zone, which has no wave requirement.

The building stock in Ortley Beach closely reflected design requirements specified in the community’s FIRM. With the X Zone having no building elevation requirement and the BFE in the AE Zone at ground level, nearly all structures in the two zones had closed foundations with an average lowest horizontal member elevation above the ground of only 0.54 m. These inadequate design standards resulted in buildings particularly vulnerable to flood damage. Structures in the X Zone determined by FEMA as only having a moderate flood risk were in fact hardest hit during Sandy due to significant wave action in the area. The average loss ratio of the 64 structures in the X Zone was 0.74. Structures in the high-risk AE Zone further inland experienced significantly less damage, with an average loss ratio of 0.17 in the flood zone. A detailed analysis of flood zones and surveyed building damage in Ortley Beach is given by Xian et al. (2015).

Following the same plotting conventions as in Fig. 9, Fig. 10a, b shows the comparison of the hindcast simulation of surge inundation and wave characteristics to flood zones from the community’s preliminary FIRM along the same transect. In the new map, the original X Zone has been narrowed and replaced with an AO Zone, which is subject to inundation by the 100-year shallow flooding event but no wave effects. Likewise, BFEs in the VE and AE Zones have been increased. Although these changes are improvements over the community’s previous FIRM, the BFE for the AE Zone is still near or at the ground level. Furthermore, the lower-risk AO Zone still covers a portion of vulnerable buildings in the community.

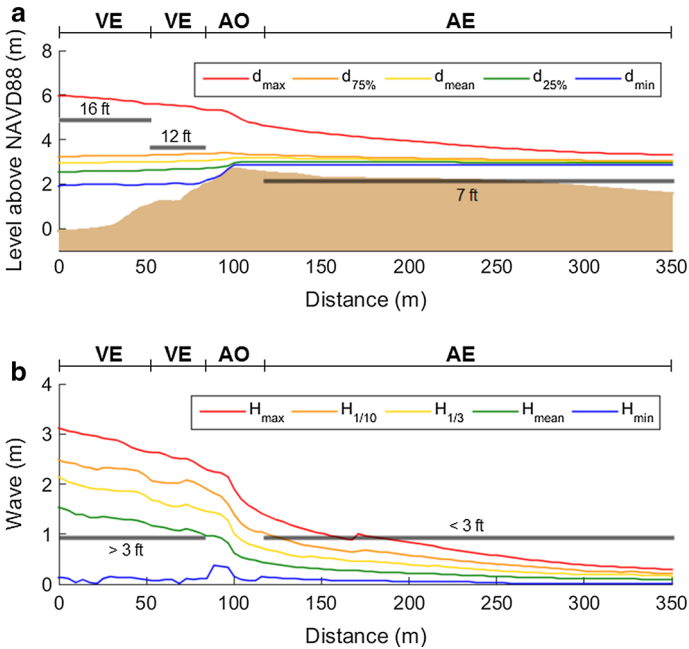


Fig. 10 Comparison of the hindcast simulation along the dashed transect shown in Fig. 2 to the preliminary effective FIRM in Ortley Beach. **a** Comparison of simulated inundation metrics to flood zone BFEs shown as horizontal black lines. The shaded brown area represents the transect’s post-Sandy ground elevation. **b** Comparison of simulated wave statistics to flood zone wave conditions

Although details from the surge analyses used to develop the effective and preliminary FIRMs are not available, it is suspected that two considerations were important to FEMA’s mapping procedure. The first consideration was the potential for back-bay flooding. Located on a narrow barrier peninsula, tidal and surge flooding in Ortley Beach from Barnegat Bay is a constant threat and was a prominent flooding source for bayside structures during Hurricane Sandy (Richard Stockton College of New Jersey 2012). As a result of this flood exposure, the effective FIRM contains an AE Zone with a 6-foot BFE extending from the bayside a kilometer inland into the study area (Fig. 9a). Since ground elevation is gradually increasing, however, this high-risk AE Zone does not extend completely to the community’s dune. This intermediate area located on slightly higher ground elevation is designated in the effective FIRM as a moderate-risk X Zone outside the 100-year floodplain.

The unexpected placement of an X Zone in the area nearest to the coast and presumably most exposed to direct surge flooding implies that significant dune erosion was not considered as probable during FEMA’s flood mapping. To assess Sandy’s impact in the case no storm-induced erosion had occurred, the transect simulation is repeated using its pre-Sandy elevation. Results (not shown) indicate that in this scenario only slight surge overtopping of the dune and minimal wave action in the community would have occurred, closely reflecting expected flood conditions in an X Zone. However, with Ortley Beach’s frontal dune eroding by nearly 3 m during Sandy, it is clear that dune reliability was not adequately considered in the community’s FIRM, leading to a significant underestimation of flood risk.

FEMA currently assesses dune performance using the so-called 540 square foot rule which deems a dune as effective if its cross-sectional area above the 100-year stillwater elevation and seaward of the dune crest is greater than 540 square feet (FEMA 2002). This simple geometric method is based on a study of 38 storms which related their estimated stillwater return levels to the eroded area of dunes (Hallermeier and Rhodes 1988). This strictly empirical approach, however, fails to account for important physical considerations such as beach morphology, sediment characteristics and storm duration among many others (MacArthur et al. 2005). As a result, the method has been shown to inconsistently predict dune erosion. In a study of dune vulnerability in North Carolina during Hurricane Fran (1996), for example, the Hallermeier and Rhodes method successfully predicted 97% of survived dunes but only 46% of failed dunes (Judge et al. 2003).

The results of the Ortley Beach analysis illustrate the importance of better understanding dune performance under surge and wave action and correctly distinguishing between flooding sources when developing flood hazard maps. The lack of redundancy in linear defenses such as dunes means that storm-induced erosion often leads to catastrophic inland flooding. Indeed, nearly all the communities in New Jersey significantly impacted by Sandy's surge also experienced some degree of dune erosion. In the case of Mantoloking, located 9 km north of Ortley Beach, erosion was so severe that storm surge breached the barrier peninsula altogether. Correctly estimating dune performance and accounting for changing reliability due to long-term erosion therefore is a critical objective. The impacts of direct coastal flooding, however, should also be correctly distinguished from secondary flood effects such as back-bay flooding. Understanding the relative exposure of a community to different flood sources is an important step toward developing flood maps which consistently reflect the community's true flood risk.

7 Conclusion

Accurately estimating structural vulnerability and reliably mapping flood hazards are both dependent on accurately modeling inland storm surge flooding. In this study, a pair of hydrodynamic models (ADCIRC + SWAN and BOUSS1D) is proposed as an effective framework for doing so. The models are applied to a case study of Hurricane Sandy and the heavily impacted community of Ortley Beach, New Jersey. Both models, respectively, show good agreement with observed storm tide gauge measurements and surveyed high-water marks in the community.

The proposed models are used to hindcast storm surge flooding in the community. Due to a topographical feature of the community where ground elevation slightly decreases with distance inland, maximum surge inundation across the community was roughly constant. In contrast, wave and velocity effects strongly dissipate with distance from the coast and are more consistent with surveyed building damage. The hindcast simulation is used to develop damage and fragility curves relating a building's expected and probable loss ratio to several surge hazard predictors. Although inundation depth is a fundamental damage predictor, it is clear that wave and hydrodynamic effects are critical damage mechanisms and thus must be considered when estimating vulnerability. This is especially true if the goal is to estimate losses due to structural damage as opposed to building content losses.

These findings provide important insight when considering structural vulnerability for other storm surge events or coastal locations. While traditional depth-damage curves are

widely available and serve as the basis for a majority of flood vulnerability studies, special care should be taken when applying them to predict building damage. Among the most important considerations is ensuring the wave environment implicitly quantified in empirical depth-damage curves is consistent with the assumptions of a particular study. To overcome this ambiguity, greater effort should be placed on estimating and applying wave and velocity-damage curves like those recommended in this study. Important potential extensions include considering various construction types and additional hazard parameters such as flood duration. Furthermore, greater numerical and experimental research into surge–structure interaction is needed in order to better characterize flood loads on structures.

The hindcast simulation is also compared with the flood risk zones from both the community’s effective FIRM during Sandy and its soon-to-be adopted FIRM. The effective FIRM is found to have significantly misrepresented the community’s flood risk by placing a moderate-risk X Zone near the coast between two high-risk zones. This strong discontinuity in flood risk was not apparent in the hindcast of inundation and wave effects. It is suspected this unexpected placement resulted from considering Barnegat Bay as the community’s primary flood source and from overestimating the reliability of the community’s coastal dune using FEMA’s simplistic ‘540 square foot rule.’ In the future, greater emphasis should be placed on assessing the reliability of coastal defenses.

Although in this study we focus on mapping inland flooding from a single historical event, the ADCIRC + SWAN and BOUSS1D framework can also be coupled with recent techniques in cyclone modeling to map inland flood with various return periods. In the absence of extensive historical storm records, recent studies have used physics-based approaches to predict the occurrence of synthetic but physically possible hurricane events in both the current and future climates (Emanuel et al. 2008; Lin et al. 2012). This technique can be used to simulate high impact extreme events which have yet to be observed due to their low probability (Lin and Emanuel 2015). Coupling the ADCIRC + SWAN and BOUSS1D models with such a database of synthetic hurricane events can be used to comprehensively study extreme inland flooding. In particular, the approach can be used to systematically communicate flood exposure by mapping return periods of surge, wave and hydrodynamic effects. These flood effects can be mapped for various return periods rather than the typical practice of mapping solely for the 100- or 500-year event. Finally, flood maps can also be developed based on projections of the future climate to quantify the impact of climate change and sea level rise (Kopp et al. 2014; Lin et al. 2016) on inland flooding.

Acknowledgements This research was supported by the National Science Foundation (NSF) Grant EAR-1520683 and the United States Army Corps of Engineers (USACE) Climate Preparedness and Resilience Program with administrative support from Oak Ridge Institute for Science and Education (ORISE). The authors would like to thank Dr. Andrew Kennedy for his helpful insights and suggestions.

Open Access This article is distributed under the terms of the Creative Commons Attribution 4.0 International License (<http://creativecommons.org/licenses/by/4.0/>), which permits unrestricted use, distribution, and reproduction in any medium, provided you give appropriate credit to the original author(s) and the source, provide a link to the Creative Commons license, and indicate if changes were made.

References

Aerts JC, Botzen WW, Emanuel K, Lin N, de Moel H, Michel-Kerjan EO (2014) Evaluating flood resilience strategies for coastal megacities. *Science* 344:473–475

- Agresti A (2010) Analysis of ordinal categorical data. Wiley series in probability and statistics, 2nd edn. Wiley, Hoboken
- Allsop W, Vicinanza D, McKenna J (1996) Wave forces on vertical and composite breakwaters. Hydraulic Research, Wallingford
- Blake ES, Kimberlain TB, Berg RJ, Cangialosi J, Beven JL II (2013) Tropical cyclone report: Hurricane Sandy (AL182012). National Hurricane Center, Miami
- Booij N, Ris R, Holthuijsen LH (1999) A third-generation wave model for coastal regions: 1. Model description and validation. *J Geophys Res Oceans* 104:7649–7666
- Botts H, Jeffery T, Du W, Suhr L (2015) CoreLogic Storm Surge Report. CoreLogic
- Chavas DR, Lin N, Emanuel K (2015) A model for the complete radial structure of the tropical cyclone wind field. Part I: comparison with observed structure. *J Atmos Sci* 72:3647–3662
- Crowell M, Hirsch E, Hayes TL (2007) Improving FEMA's coastal risk assessment through the National Flood Insurance Program: an historical overview. *Mar Technol Soc J* 41:18–27
- Davis SA, Skaggs LL (1992) Catalog of residential depth-damage functions used by the Army Corps of Engineers in flood damage estimations (IWR Report 92-R-3). United States Army Corps of Engineers, Washington
- Davis SA, Johnson ND, Hansen WJ, Reynolds FR Jr, Warren J, Foley CO, Fulton RL (1988) National economic development procedures manual: urban flood damage (IWR Report 88-R-2). United States Army Corps of Engineers, Washington
- Demirbilek Z, Nwogu OG, Ward DL, Sanchez A (2009) Wave transformation over reefs: evaluation of one-dimensional numerical models. United States Army Engineering Research and Development Center, Vicksburg
- Demuth JL, DeMaria M, Knaff JA (2006) Improvement of advanced microwave sounding unit tropical cyclone intensity and size estimation algorithms. *J Appl Meteorol Clim* 45:1573–1581
- Dietrich JC et al (2011) Modeling hurricane waves and storm surge using integrally-coupled, scalable computations. *Coast Eng* 58:45–65
- Dietrich JC et al (2012) Performance of the unstructured-mesh, SWAN + ADCIRC model in computing hurricane waves and surge. *J Sci Comput* 52:468–497
- Divoky D, Battalio R, Dean B, Collins I, Hatheway D, Scheffner N (2005) Storm meteorology: FEMA coastal flood hazard analysis and mapping guidelines. Federal Emergency Management Agency, Washington
- Emanuel K, Sundararajan R, Williams J (2008) Hurricanes and global warming: results from downscaling IPCC AR4 simulations. *Bull Am Meteorol Soc* 89:347–367
- FEMA (2002) Appendix D: guidance for coastal flooding analyses and mapping
- FEMA (2010) Substantial improvement/substantial damage desk reference (FEMA P-758)
- FEMA (2011) Coastal construction manual (FEMA P-55)
- FEMA (2013) Hurricane Sandy in New Jersey and New York (FEMA P-942)
- FEMA (2014a) Flood insurance study: ocean county, New Jersey
- FEMA (2014b) Region II coastal storm surge study: overview
- Fletcher C, Richmond B, Barnes G, Schroeder T (1995) Marine flooding on the coast of Kaua'i during Hurricane Iniki: hindcasting inundation components and delineating washover. *J Coast Res* 11:188–204
- Forristall GZ (1978) On the statistical distribution of wave heights in a storm. *J Geophys Res Oceans* 83:2353–2358
- Government Accountability Office (2015) Report to congressional committees. Government Accountability Office, Washington
- Hallegatte S, Green C, Nicholls RJ, Corfee-Morlot J (2013) Future flood losses in major coastal cities. *Nat Clim Change* 3:802–806
- Hallermeier RJ, Rhodes PE (1988) Generic treatment of dune erosion for 100-year event. In: 21st international conference on coastal engineering, Costa del Sol-Malaga, Spain, pp 1197–1211
- Halverson JB, Rabenhorst T (2013) Hurricane Sandy: the science and impacts of a Superstorm. *Weatherwise* 66:14–23
- Hasselmann K et al (1973) Measurements of wind-wave growth and swell decay during the Joint North Sea Wave Project (JONSWAP). Deutsches Hydrographisches Institut, Hamburg
- Hatheway D, Coulton K, DelCharco M, Jones C (2005) Flood hazard zones. Federal Emergency Management Agency, Washington
- Hatzikyriakou A, Lin N (2016) Impact of performance interdependencies on structural vulnerability: a systems perspective of storm surge risk to coastal residential communities. *Reliab Eng Syst Saf* 158:106–116

- Hatzikyriakou A, Lin N, Gong J, Xian S, Hu X, Kennedy A (2015) Component-based vulnerability analysis for residential structures subjected to storm surge impact from Hurricane Sandy. *Nat Hazards Rev*. doi:[10.1061/\(ASCE\)NH.1527-6996.0000205](https://doi.org/10.1061/(ASCE)NH.1527-6996.0000205)
- Holland GJ (1980) An analytic model of the wind and pressure profiles in hurricanes. *Mon Weather Rev* 108:1212–1218
- Judge EK, Overton MF, Fisher JS (2003) Vulnerability indicators for coastal dunes. *J Waterw Port Coast Ocean Eng* 129:270–278
- Kennedy AB et al (2012) Tropical cyclone inundation potential on the Hawaiian Islands of Oahu and Kauai. *Ocean Model* 52–53:54–68
- Kopp RE et al (2014) Probabilistic 21st and 22nd century sea-level projections at a global network of tide-gauge sites. *Earth's Future* 2:383–406
- Lin N, Chavas D (2012) On hurricane parametric wind and applications in storm surge modeling. *J Geophys Res*. doi:[10.1029/2011JD017126](https://doi.org/10.1029/2011JD017126)
- Lin N, Emanuel K (2015) Grey swan tropical cyclones. *Nat Clim Change* 6:106–111
- Lin N, Emanuel K, Oppenheimer M, Vanmarcke E (2012) Physically based assessment of hurricane surge threat under climate change. *Nat Clim Change* 2:462–467
- Lin N, Kopp RE, Horton BP, Donnelly JP (2016) Hurricane Sandy's flood frequency increasing from year 1800 to 2100. *Proc Natl Acad Sci* 113:12071–12075
- Luetlich R, Westerink J, Scheffner NW (1992) ADCIRC: an advanced three-dimensional circulation model for shelves, coasts, and estuaries. Report 1. Theory and methodology of ADCIRC-2DDI and ADCIRC-3DL
- MacArthur B et al (2005) Event-based erosion: FEMA coastal flood hazard analysis and mapping guidelines. Federal Emergency Management Agency, Washington
- Mattingly KS, McLeod JT, Knox JA, Shepherd JM, Mote TL (2014) A climatological assessment of Greenland blocking conditions associated with the track of Hurricane Sandy and historical North Atlantic hurricanes. *Int J Climatol* 35:746–760
- McCallum BE et al (2013) Monitoring storm tide and flooding from Hurricane Sandy along the Atlantic coast of the United States, October 2012. United States Geological Survey, Reston
- Merz B, Thielen AH, Gocht M (2007) Flood risk mapping at the local scale: concepts and challenges. In: Begum S, Stive MJF, Hall JW (eds) *Flood risk management in Europe: innovation in policy and practice*. Springer, Dordrecht
- National Research Council (2009) Mapping the zone: improving flood map accuracy. National Academy of Sciences, Washington
- O'Dea C (2013) Interactive map: assessing damage from Superstorm Sandy. <http://www.njspotlight.com/stories/13/03/14/assessing-damage-from-superstorm-sandy/>. Accessed April 22, 2015
- Ospina R, Ferrari SLP (2008) Inflated beta distributions. *Stat Pap* 51:111–126
- Papke LE, Wooldridge JM (1996) Econometric methods for fractional response variables with an application to 401 (K) plan participation rates. *J Appl Econom* 11:619–632
- R Development Core Team (2015) R: a language and environment for statistical computing. R Foundation for Statistical Computing, Vienna
- RS Means (2013) RS Means Online Database. <http://www.rsmeansonline.com/>
- Ramalho EA, Ramalho JJ, Henriques PD (2010) Fractional regression models for second stage DEA efficiency analyses. *J Prod Anal* 34:239–255
- Ramalho EA, Ramalho JJ, Murteira JM (2011) Alternative estimating and testing empirical strategies for fractional regression models. *J Econ Surv* 25:19–68
- Richard Stockton College of New Jersey (2012) Barnegat Bay storm surge elevations during Hurricane Sandy and sources of surge flooding within the bay. The Coastal Research Center, Port Republic
- Scawthorn C et al (2006) HAZUS-MH flood loss estimation methodology: II. Damage and loss assessment. *Nat Hazards Rev* 7:72–81
- Suppasri A, Koshimura S, Imamura F (2011) Developing tsunami fragility curves based on the satellite remote sensing and the numerical modeling of the 2004 Indian Ocean tsunami in Thailand. *Nat Hazard Earth Syst* 11:173–189
- Tafanidis A, Kennedy A, Westerink J, Smith J, Cheung K, Hope M, Tanaka S (2013) Rapid assessment of wave and surge risk during landfalling hurricanes: probabilistic approach. *J Waterw Port Coast Ocean Eng* 139:171–182
- Tomiczek T, Kennedy A, Rogers S (2014) Collapse limit state fragilities of wood-framed residences from storm surge and waves during Hurricane Ike. *J Waterw Port Coast Ocean Eng* 140:43–55
- Tomiczek T, Kennedy A, Zhang Y, Owensby M, Hope M, Lin N, Flores A (2017) Hurricane damage classification methodology and fragility functions derived from Hurricane Sandy's effects in coastal New Jersey. *J Waterw Port Coast Ocean Eng* 143:04017027

- Walton T, Ahrens J, Truitt C, Dean R (1989) Criteria for evaluating coastal flood-protection structures. United States Army Corps of Engineers, Washington
- Warton DI, Hui FK (2011) The arcsine is asinine: the analysis of proportions in ecology. *Ecology* 92:3–10
- Wetmore F et al (2016) An evaluation of the National Flood Insurance Program. American Institutes for Research, Washington
- Wright CW, Fredericks X, Troche RJ, Klipp ES, Kranenburg CJ, Nagle DB (2014) EAARL-B coastal topography—Eastern New Jersey, Hurricane Sandy, 2012. United States Geological Survey, Reston
- Xian S, Lin N, Hatzikyriakou A (2015) Storm surge damage to residential areas: a quantitative analysis for Hurricane Sandy in comparison with FEMA flood map. *Nat Hazards* 79:1867–1888
- Yin J, Lin N, Yu D (2016) Coupled modeling of storm surge and coastal inundation: a case study in New York City during Hurricane Sandy. *Water Resour Res* 52:8685–8699